Sideslip Angle Estimation Using GPS and Disturbance Accommodating Multi-rate Kalman Filter for Electric Vehicle Stability Control

Binh Minh Nguyen[1], Yafei Wang[2], Hiroshi Fujimoto[1], Yoichi Hori[1]
[1]Department of Advanced Energy, the University of Tokyo, Japan
[2]Department of Electrical Engineering, the University of Tokyo, Japan
E-mail: minh@hori.k.u-tokyo.ac.jp, wang@hori.k.u-tokyo.ac.jp, fujimoto@k.u.tokyo.ac.jp, hori@k.u-tokyo.ac.jp

***Abstract*-This paper describes a new method of sideslip angle estimation for electric vehicle stability control system. Multi-rate Kalman filter is designed based on the measurements of yaw rate (updated every 1 ms) and course angle from GPS receiver (updated every 200 ms). By disturbance accommodating method, robust estimation of sideslip angle is achieved. Direct yaw moment generated by in-wheel motors' torque is used to control both yaw rate and sideslip angle of electric vehicle. Experiments are conducted to verify the effectiveness of the proposal.**

***Keywords*-Sideslip angle, Kalman filter, multi-rate, electric vehicle, GPS**

I. INTRODUCTION

Due to environmental protection and energy conservation, electric vehicles (EVs) have been interested by both industry and academic circles. Driven by electric motors, EVs have remarkable advantages in comparison with internal combustion engine vehicles (ICEVs) [1]. Firstly, compact electric motors can be installed at each wheel. This feature enables independent torque control at each wheel for vehicle stability control system [2]. Secondly, EVs' torque response is 10-100 times faster than that of ICEVs. Last but not least, motor torque can be measured easily based on motor currents.

Vehicle stability control (VSC) based on active safety technologies is a big issue in motion control of EVs. In VSC system, both yaw rate and sideslip angle at the center of gravity must be measured or estimated to be compared with the reference values calculated from driver's inputs [3]. While yaw rate can be measured easily from gyroscope, current EVs are not equipped with an ability of measuring sideslip angle directly. Corrsys-Datron produces the noncontact optical sensor for sideslip angle calculation based on lateral and longitudinal velocity measurement [4]. However, due to its very high cost, Corrsys-Datron sensor cannot be a practical solution. In order to reduce the cost and improve the safety of the EV system, it is very important to design the sideslip angle estimation.

Conventional sideslip angle estimation methods using accelerometers can be categorized into three groups: kinematic based estimation [5], nonlinear dynamics model based estimation [6] [7], and linear dynamics model based estimation [8] [9]. Due to the use of lateral acceleration as one measurement, cornering stiffness appears in the output measurement equation. In fact, cornering stiffness varies with the change of road condition. This introduces error to estimation model. Moreover, the measurement of lateral acceleration is influenced by gravity on bank road, and the wind effect is also not properly captured.

Visual information can provide the heading angle of vehicle for sideslip angle estimation design [10]. However, the poor update rate of camera information is the main disadvantages of this approach. Moreover, camera visibility may be unavailable when road makers are covered with leaves, snow, water, or dirt.

By placing two GPS antenna at two points along vehicle, sideslip angle can be calculated [11]. One GPS antenna can be combined with linear model based to estimate both sideslip angle and yaw angle using Kalman filter [12]. Like vision-based method, the main problem of GPS-based estimation is the low update rate of GPS receiver (1-10 Hz) which is not fast enough for motion control system. The robustness of estimation using GPS over the variation of cornering stiffness and external disturbances was not considered in [12]. Moreover, the authors of [12] did not implement the estimation model in vehicle control system.

Japan's own GPS system has been constructed as national projects. This promising scenario enables the high accuracy of vehicle motion measurement based on GPS. In this paper, the application of GPS in sideslip angle estimation for VSC system of EVs is proposed. Multi-rate Kalman filter is designed using the measurement of yaw rate (sampling time of 1 ms) and course angle from GPS receiver (sampling time of 200 ms). By treating the combination of model uncertainties and external disturbances as extended states to be estimated, high robustness of estimation is achieved. This is the principle of disturbance accommodating control which was firstly proposed in [13]. The remainder of this paper is constructed as follows: Section II introduces the modeling of EV dynamics. The proposed estimation method is presented in section III. In section IV, the VSC system of EVs is designed by using direct yaw moment control based on linear quadratic regulator. Experiment results are demonstrated in section V. Finally, conclusions and future works are given in section VI.

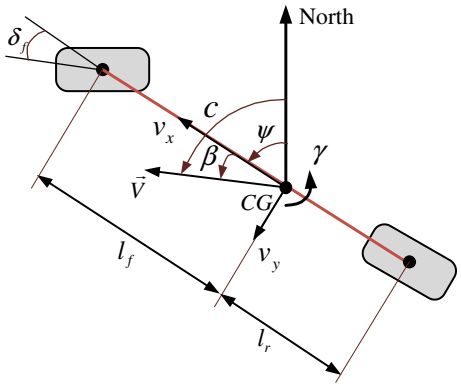

Fig. 1. Planar bicycle model of electric vehicle.

TABLE I
NOMENCLATURES

l_f, l_r	Distances from front (rear) axle to center of gravity
C_f, C_r	Front (rear) cornering stiffness
I_z	Yaw moment of inertia
δ_f	Front steering angle
N_z	Yaw moment generated by in-wheel motors
M	Vehicle mass
β	Sideslip angle
γ	Yaw rate
ψ	Yaw angle
c	Course angle obtained from GPS
v_x	Longitudinal velocity
v_y	Lateral velocity
V	Velocity vector

II. MODELING OF VEHICLE DYNAMICS

The vehicle model used in this paper is the planar bicycle model which is shown in Fig. 1. Sideslip angle is defined as the angle between velocity vector and longitudinal direction. Course angle of a moving vehicle is defined as the angle between vehicle's direction and geodetic North. Using this definition, course angle can be represented as the summary of yaw angle and sideslip angle. The influence of external disturbances can be generalized by the lateral force F_d and yaw moment N_d. Vehicle dynamics can be expressed by the following equations.

$$Mv_x\left(\dot{\beta}+\gamma\right)=-2C_f\left(\beta+\frac{l_f\gamma}{v_x}-\delta_f\right)-2C_r\left(\beta-\frac{l_r\gamma}{v_x}\right)+F_d \quad (1)$$

$$I_z\dot{\gamma}=-2C_f\left(\beta+\frac{l_f\gamma}{v_x}-\delta_f\right)l_f+2C_r\left(\beta-\frac{l_r\gamma}{v_x}\right)l_r + N_z+N_d \quad (2)$$

$$c=\psi+\beta \quad (3)$$

Cornering stiffness are represented by the summary of the nominal terms C_{fn}, C_{rn} and the variation terms $\triangle C_f$, $\triangle C_r$. From (1), (2), and (3), the state space model of vehicle dynamics are expressed as (4) with unknown input terms d_1 and d_2. The unknown input terms represented the general influence of both model uncertainties and external disturbances.

$$\dot{x}=A_n x+B_n u+Dd \quad (4)$$

Where

$$x=\begin{bmatrix}\beta & \gamma & \psi\end{bmatrix}^T,\ u=\begin{bmatrix}\delta_f & N_z\end{bmatrix}^T,\ d=\begin{bmatrix}d_1 & d_2\end{bmatrix}^T \quad (5)$$

$$A_n=\begin{bmatrix}\frac{-2\left(C_{fn}+C_{rn}\right)}{Mv_x} & -1-\frac{2\left(C_{fn}l_f-C_{rn}l_r\right)}{Mv_x^2} & 0\\ \frac{-2\left(C_{fn}l_f-C_{rn}l_r\right)}{I_z} & \frac{-2\left(C_{fn}l_f^2+C_{rn}l_r^2\right)}{I_z v_x} & 0\\ 0 & 1 & 0\end{bmatrix} \quad (6)$$

$$B_n=\begin{bmatrix}\frac{2C_{fn}}{Mv_x} & 0\\ \frac{2C_{fn}l_f}{I_z} & \frac{1}{I_z}\\ 0 & 0\end{bmatrix},\ D=\begin{bmatrix}1 & 0\\ 0 & 1\\ 0 & 0\end{bmatrix} \quad (7)$$

$$d_1=\frac{-2\left(\Delta C_f+\Delta C_r\right)}{Mv_x}\beta+\frac{-2\left(\Delta C_f l_f-\Delta C_r l_r\right)}{Mv_x^2}\gamma + \frac{2\Delta C_f}{Mv_x}\delta_f+\frac{1}{Mv_x}F_d \quad (8)$$

$$d_2=\frac{-2\left(\Delta C_f l_f-\Delta C_r l_r\right)}{I_z}\beta+\frac{-2\left(\Delta C_f l_f^2+\Delta C_r l_r^2\right)}{I_z v_x}\gamma + \frac{2\Delta C_f l_f}{I_z}\delta_f+\frac{1}{I_z}N_d \quad (9)$$

III. SIDESLIP ANGLE ESTIMATION DESIGN

A. *Disturbance Accommodating*

In this section, the idea of disturbance accommodating [13] is applied for robust estimation of sideslip angle. The continuous model (4) is transformed to the discrete model (10) with process noise w_k by using the transformation (11). T_c is the fundamental sampling time which is 1 ms in this paper, and I is the unity matrix.

$$x_{k+1}=A_{nd,k}x_k+B_{nd,k}u_k+D\left(T_c I\right)d_k+w_k \quad (10)$$

$$A_{nd,k}=e^{A_n T_c}\approx A_n\left(T_c I\right)+I,\ B_{nd,k}=\int_0^{T_c}e^{A_n\tau}d\tau B_n\approx B_n\left(T_c I\right) \quad (11)$$

In order to compensate the influence of unknown input terms, we treat d_k as a stochastic process with the dynamics expressed in (12) where w_{dk} is a zero-mean white noise sequence.

$$d_{k+1} = d_k + w_{d,k} \tag{12}$$

The key idea of this paper is the introduction of the unknown disturbance d_k as extended states. The new state vector h_k and the new state space model with new process noise $w_{new,k}$ are constructed as follows:

$$h_k = \begin{bmatrix} \beta_k & \gamma_k & \psi_k & d_{1,k} & d_{2,k} \end{bmatrix}^T \tag{13}$$

$$h_{k+1} = K_{nd,k} h_k + G_{nd,k} u_k + w_{new,k} \tag{14}$$

$$K_{nd,k} = \begin{bmatrix} A_{nd,k} & T_c I \\ 0 & I \end{bmatrix}, G_{nd,k} = \begin{bmatrix} B_{nd,k} \\ 0 \end{bmatrix} \tag{15}$$

B. Output Measurements

Yaw rate and course angle are selected as output measurements for Kalman filter design. While yaw rate measurement can be sampled at T_c (1 ms), the measurement of course angle from GPS receiver is updated every $T_s > T_c$ (200 ms in this study). The estimation step between two continuous updates of course angle is named "inter-samples" as shown in Fig. 2. During inter-samples, there is no course angle update. Output measurement equation is expressed in (16) where v_k is the measurement noise. Measurement matrix Z_k is constructed as (17) and (18).

$$y_k = Z_k h_k + v_k \tag{16}$$

If course angle is updated ($k = T_s/T_c$):

$$Z_k = \begin{bmatrix} 0 & 1 & 0 & 0 & 0 \\ 1 & 0 & 1 & 0 & 0 \end{bmatrix} \tag{17}$$

During inter-samples ($k \neq T_s/T_c$):

$$Z_k = \begin{bmatrix} 0 & 1 & 0 & 0 & 0 \\ 0 & 0 & 0 & 0 & 0 \end{bmatrix} \tag{18}$$

C. Kalman Filter Algorithm

The model for estimation includes the dynamics equation as (13) and output measurement equation as (16). Q_w and Q_v are the process noise and measurement noise covariance matrices. They are tuning parameters of the Kalman filter algorithm shown in Fig. 3. If Q_v is too large, the Kalman gain decreases, thus, the estimation fails to update the propagated disturbances based on measurements. As in (19), σ_{γ_gyro} and σ_{c_GPS} denote the variance of yaw rate noise and course angle noise, respectively. They are chosen based on the idea that measurement of course angle is more reliable than measurement of yaw rate. Small Q_w results in unstable estimation. On the other hand, large Q_w forces the estimation to completely rely upon the measurements.

$$Q_v = \begin{bmatrix} \sigma^2_{\gamma\_gyro} & 0 \\ 0 & \sigma^2_{c\_GPS} \end{bmatrix} \tag{19}$$

$$Q_w = \begin{bmatrix} q_{11}^2 & 0 & 0 & 0 & 0 \\ 0 & q_{22}^2 & 0 & 0 & 0 \\ 0 & 0 & q_{33}^2 & 0 & 0 \\ 0 & 0 & 0 & q_{44}^2 & 0 \\ 0 & 0 & 0 & 0 & q_{55}^2 \end{bmatrix} \tag{20}$$

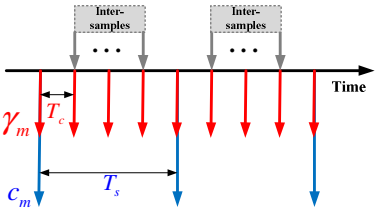

Fig. 2. Two sampling times of output measurements.

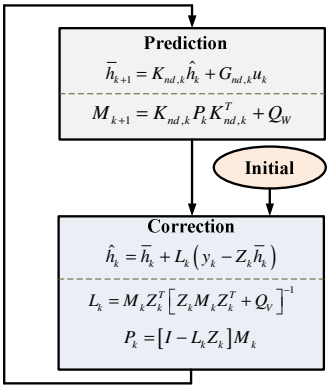

Fig. 3. Kalman filter algorithm for sideslip angle estimation.

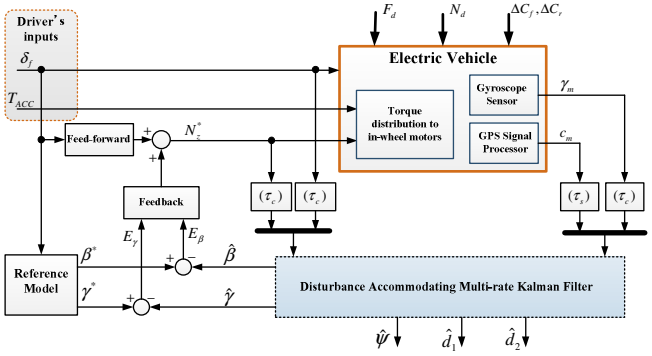

Fig. 4. Electric vehicle stability control system using GPS.

IV. STABILITY CONTROL SYSTEM DESIGN

The general VSC of electric vehicle is shown in Fig. 4. The reference model is designed based on the steady-state response of sideslip angle and yaw rate using the linear bicycle model in section II. The following equations express the calculation of reference values from driver's steering angle.

$$\beta^* = G_\beta(s)\delta_f = \frac{\left[1 - \frac{M}{2(l_f + l_r)}\frac{l_f}{C_{rn} l_r} v_x^2\right]\frac{l_r}{(l_f + l_r)}\frac{\delta_f}{1 + \tau_\beta s}}{1 - \frac{M}{2(l_f + l_r)^2}\frac{C_{fn} l_f - C_{rn} l_r}{C_{fn} C_{rn}} v_x^2} \tag{21}$$

$$\gamma^* = G_\gamma(s)\delta_f = \frac{\frac{v_x}{(l_f + l_r)}\frac{\delta_f}{1 + \tau_\gamma}}{1 - \frac{M}{2(l_f + l_r)^2}\frac{C_{fn} l_f - C_{rn} l_r}{C_{fn} C_{rn}} v_x^2} \tag{22}$$

In this paper, only yaw moment generated by in-wheel motors is selected as control input. From (1) and (2), sideslip angle can be derived from front steering angle and yaw moment as follows:

$$\beta = G_{11}(s)\delta_f + G_{12}(s)N_z \tag{23}$$

In this study, in order to demonstrate the estimation and control of sideslip angle, the feed-forward control is designed in order to track the sideslip angle response with its reference value. From (21) and (23), the transfer function of feed-forward controller is designed as:

$$G_{ff}(s) = \frac{G_\beta(s) - G_{11}(s)}{G_{12}(s)} \tag{24}$$

In order to minimize the tracking error, linear quadratic regulator (LQR) is applied in feedback controller. The yaw moment control is designed as follows:

$$N_z^* = g_\beta E_\beta + g_\gamma E_\gamma = g_\beta\left(\beta^* - \hat{\beta}\right) + g_\gamma\left(\gamma^* - \hat{\gamma}\right) \tag{25}$$

The feedback gains are determined by minimizing the following cost function J:

$$J = \frac{1}{2}\int_0^\infty \left[q_\beta\left(\beta^* - \hat{\beta}\right)^2 + q_\gamma\left(\gamma^* - \hat{\gamma}\right)^2 + q_N\left(N_z^*\right)^2 \right] dt \tag{26}$$

In (26), the weighting factors q_β, q_γ, and q_N are chosen by the size of state and control input limitation. Because there is only one control input, there is a "trade-off" between sideslip angle control and yaw rate control. Because sideslip angle is very sensitive to the stability of vehicle, it is given bigger weight in this study.

V. EXPERIMENT

A. Experiment Setup

A one seat micro EV named "Super-capacitor COMS" is used for experiment in this paper (Fig. 5). Two in-wheel motors are equipped in the rear wheels. Other sensors are steering angle sensor, longitudinal and lateral acceleration sensor, and gyroscope for yaw rate measurement. In order to measure the sideslip angle, a Corrsys-Datron optical sensor is installed in the front of the vehicle. Using the lateral and longitudinal velocity measured by this optical sensor, sideslip angle at the center of gravity is obtained. A RT-Linux operating system PC is used as the controller of COMS1 with the control period of 1 millisecond.

GPS receiver CCA-600 supported by Japan Radio Co., Ltd is used in this study. It can provide the measurement of course angle at 5 Hz update rate with the accuracy of 0.14 degree RMS which is better than the one used at Stanford University (course angle accuracy of 0.25 degree RMS) for the research in [11]. In order to transfer the data from CCA-600 to the experimental electric vehicle, GPS interface software is designed in a laptop (Fig. 6). It receives the NMEA messages from CCA-600 through serial port. Then, it decodes the NMEA messages. The decoded data is sent to EV's controller through LAN cable by user datagram protocol (UDP). Data recorded by GPS interface including vehicle course angle during an experiment is shown in Fig. 7.

Fig. 5. Electric vehicle COMS.

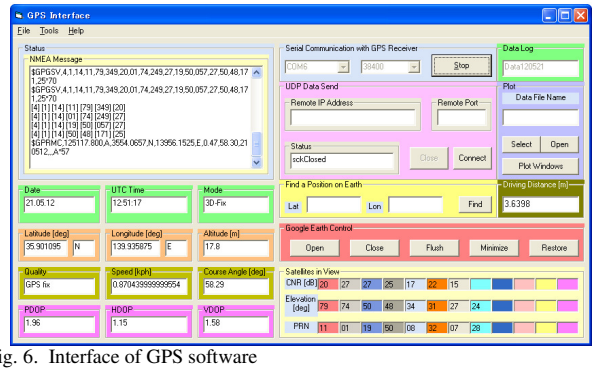

Fig. 6. Interface of GPS software

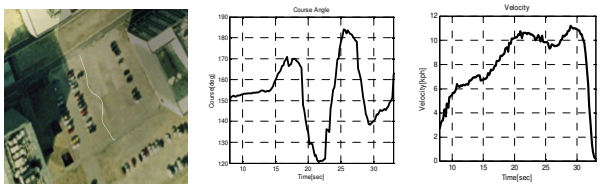

(a) (b) (c)

Fig. 7 Data recorded by GPS interface:
(a) vehicle position, (b) course angle (c) velocity

TABLE II
ESTIMATION METHODS

Method	Estimated states	Output measurements
SRKF	$[\beta \quad \gamma]^T$	γ
MRKF	$[\beta \quad \gamma \quad \psi]^T$	$[\gamma \quad c]^T$
DACMRKF	$[\beta \quad \gamma \quad \psi \quad d_1 \quad d_2]^T$	$[\gamma \quad c]^T$

B. Experiment results

1. State estimation results

In order to demonstrate the effectiveness of the proposed disturbance accommodating multi-rate Kalman filter (DACMRKF), other two estimation methods are performed for comparing: multi-rate Kalman filter (MRKF) and single-rate Kalman filter (SRKF). The features of each estimation methods are shown in TABLE II. Two experiment modes are conducted: lane-change test and cornering test. Tests are conducted on high friction road (asphalt, μ = 0.8) at the speed of 20 kph. The true cornering stiffness on this road condition is C_f = 10,000 [*N/rad*] and C_r = 10,000 [*N/rad*]. The nominal cornering stiffness of estimation model is set as: C_{fn} = 7000

[*N/rad*] and C_m = 7000 [*N/rad*]. This means a model error of cornering stiffness is introduced to estimation model. During the test, unknown external disturbances such as wind force may affect the vehicle COMS.

Results of sideslip angle estimation in lane-change test are shown in Fig. 8 (a). In Fig. 8 (b), the inter-sample performances can be seen clearly. Under model error and external disturbances, SRKF has the biggest estimation error in comparison with the real value obtain from Corrsys-Datron optical sensor. Thanks to the GPS, MRKF has the better estimation performance. When course angle is updated, estimation error is minimized. However, during inter-samples where there is no update of course angle, MRKF is degraded. Fig. 8 (c) and Fig. 8 (d) show the estimation of the unknown disturbance terms, d_1 and d_2, respectively. Because of the estimation of disturbances, DACMRKF shows the best sideslip angle estimation, even during inter-samples.

Results of cornering-test are shown in Fig. 9 (a) – Fig. 9 (d). The results represent the same conclusions as lane-change test: DACMRKF ranks first in the estimation performance. The root-mean-square deviation (RMSD) of each estimation method are calculated and summarized in TABLE III.

2. *State control results*

Cornering test is conducted on high friction road (asphalt) at the speed of 20 kph in two cases: without control, and with direct yaw moment control. In case of without control, the responses of both yaw rate and sideslip angle cannot track with the reference values (Fig. 10 (a) and Fig. 10 (b)). In contrast, when direct yaw moment control is applied, yaw rate and sideslip angle can follow the references (Fig. 11 (a) and Fig. 11 (b)). Because there is only one control input but two states, perfect tracking to the desired values cannot be achieved. Even though, the experiment results show the effect of the proposed control system in vehicle stability enhancement.

VI. CONCLUSIONS

Thanks to GPS, course angle is obtained to be an output measurement for sideslip angle estimation using multi-rate Kalman filter. However, the estimation performance of MRKF may be degraded during inter-samples due to the fact that there is no course angle update. By applying the idea of disturbance accommodating, the influences of model uncertainties and unknown external disturbances to state estimation are compensated. As a result, robust estimation of sideslip angle is achieved for VSC of EVs. The proposed method is successfully implemented in the stability control system of electric vehicles. Experiments are conducted to demonstrate the effectiveness of DACMRKF. In future works, the auto-turning of process noise and measurement noise covariance will be considered. We will also implement the active steering control together with yaw moment control. In this paper, only robust estimation is demonstrated. The feedback of estimated disturbances will be utilized for enhancing the robustness of the whole control system.

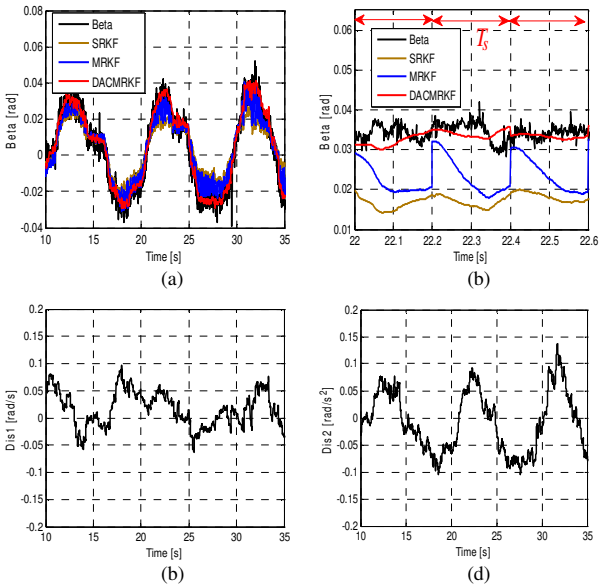

Fig. 8. Estimation results of lane-change test:
(a)sideslip angle estimation, (b) inter-sample performance, (c) estimation of disturbance term d_1, (d) estimation of disturbance term d_2.

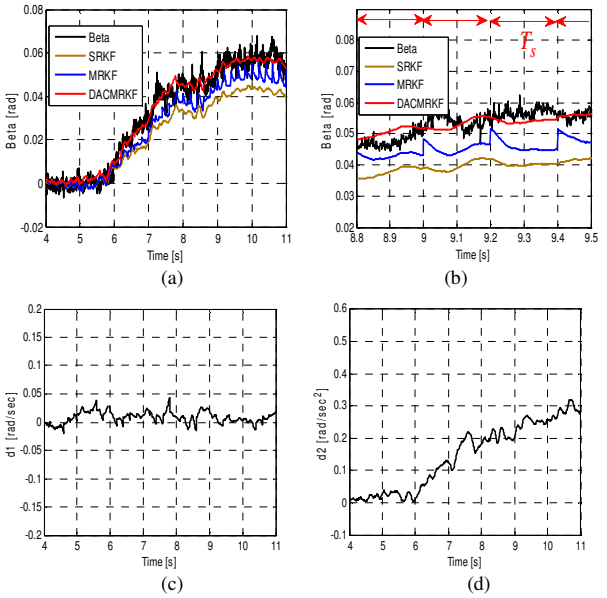

Fig. 9. Estimation results of cornering test:
(a)sideslip angle estimation, (b) inter-sample performance, (c) estimation of disturbance term d_1, (d) estimation of disturbance term d_2.

TABLE III
RMSD OF SIDESLIP ANGLE ESTIMATION

Method	**RMDS [rad]**	
	Lane-change	**Cornering**
SRKF	1.02×10^{-2}	1.12×10^{-2}
MRKF	0.86×10^{-2}	0.87×10^{-2}
DACMRKF	0.38×10^{-2}	0.41×10^{-2}

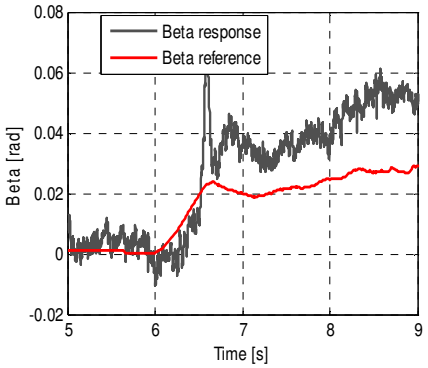

(a)

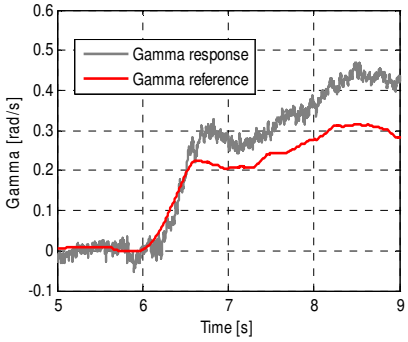

(b)

Fig. 10. Without control: (a) Sideslip angle, (b) Yaw rate.

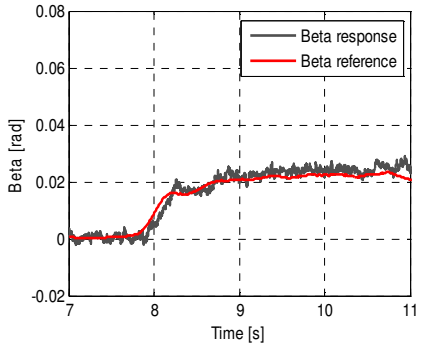

(a)

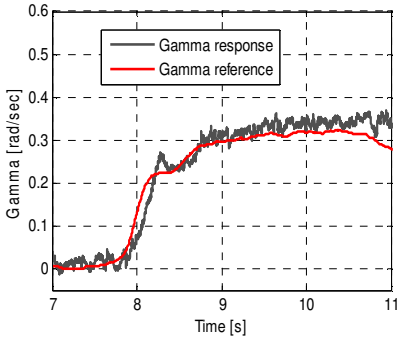

(b)

Fig. 11. With yaw moment control: (a) Sideslip angle, (b) Yaw rate.

ACKNOWLEDGEMENT

The authors would like to thank Japan Radio Company (JRC) for their supports of GPS receiver for experiments in this study.

REFERENCES

[1] Y. Hori, "Future Vehicle Driven By Electricity and Control-Research on 4 Wheel Motored UOT March II," *IEEE Transactions on Industrial Electronics*, Vol. 51, No. 5, pp. 954-962, 2004.

[2] H. Fujimoto, A. Tsumasaka, and T. Noguchi, "Direct Yaw Moment Control of Electric Vehicle Based on Cornering Stiffness Estimation," 31st IEEE Annual Conference on Industrial Electronics, pp. 2626-2631, 2005.

[3] J. Y. Wong, "Theory of Ground Vehicles," John Wiley & Sons, INC, Third Edition, 2001.

[4] Corrsys-Datron: http://www.corrsys-datron.com/optical_sensor.htm

[5] B. C. Chen and F. C. Hsieh, "Sideslip Angle Estimation Using Extended Kalman Filter," *Vehicle System Dynamics*, Vol. 46, No. 1, pp. 353-364, 2008.

[6] L. Imsland, T. A. Johansen, T. I. Fossen, H. F. Grip, J. C. Kalkkuhl, and A. Suissa, "Vehicle Velocity Estimation Using Nonlinear Observers," *Automatica*, Vol. 42, No. 12, pp. 2091-2103, 2006.

[7] M. Stria and M. C. Best, "State Estimation of Vehicle Handling Dynamics Using Non-linear Robust Extended Adaptive Kalman Filter," *Vehicle System Dynamics*, Vol. 41, pp. 103-112, 2004.

[8] Y. Aoki, T. Inoue, and Y. Hori, "Robust Design of Gain Matrix of Body Slip Angle Observer for Electric Vehicles and Its Experimental Demonstration," *8th IEEE International Workshop on Advanced Motion Control*, pp. 41-45, 2004.

[9] C. Geng, L. Mostefai, M. Denai, and Y. Hori, "Direct Yaw Moment Control of an In Wheel Motored Electric Vehicle Based on Body Slip Angle Fuzzy Observer," *IEEE Transactions on Industrial Electronics*,Vol. 56, pp.1411-1419, 2009.

[10] J. Kosecka, R. Blasi, C. J. Taylor, and J. Malik, "Vison Based Lateral Control of Vehicles," *International IEEE Conference on Intelligent Transportation System*, pp. 900-905, 1997.

[11] D. M. Bevly, J. Ryu, and J. C. Gerdes, "Integrating INS Sensors With GPS Measurements for Continuous Estimation of Vehicle Sideslip, Roll, and Tire Cornering Stiffness," *IEEE Transactions on Intelligent Transportation System*, Vol. 7, No. 4, pp. 483-493, 2006.

[12] R. Anderson and D. M. Bevly, "Estimation of Slip Angles Using A Model Based Estimator and GPS," *American Control Conference*, Vo. 3, pp. 2122-2127, 2004.

[13] C. Johnson, "Accommodation of External Disturbances in Linear Regulator and Servomechanism Problem," *IEEE Transaction on Automatic Control*, Vol. 16, No. 6, pp. 535-644, 1971.